Article:
Lin, J Y, Tallents, G J, Demir, A et al. (1998) Optimization of double drive pulse pumping in Ne-like Ge x-ray lasers. Journal of Applied Physics. pp. 1863-1868. ISSN: 1089-7550

https://doi.org/10.1063/1.366910

Optimization of double drive pulse pumping in Ne-like Ge x-ray lasers

J. Y. Lin,[a] G. J. Tallents, and A. Demir[b]
Department of Physics, University of Essex, Colchester CO4 3SQ, United Kingdom

S. B. Healy and G. J. Pert
Department of Physics, York University, York YO1 5DD, United Kingdom

(Received 13 May 1997; accepted for publication 5 November 1997)

Pumping of the Ne-like Ge x-ray laser with two 100 ps duration pulses (a prepulse and main pulse) is investigated using a fluid and atomic physics code coupled to a 3D ray tracing postprocessor code. The modeling predicts the optimum ratio of the irradiance of the two pulses for the maximum x-ray laser output resulting from the balance between the relative lower electron density gradients and wider gain region which is produced with a larger prepulse and the higher peak gain coefficients produced with a small prepulse. With a longer pulse interval between prepulse and main pulse, a relatively lower optimum pulse ratio is found. The threshold irradiance of the main driving pulse with a prepulse required to make an order of magnitude enhancement of laser output compared to irradiation without a prepulse is also found at $3-4\times10^{13}$ W/cm^2 for Ne-like Ge. © *1998 American Institute of Physics.* [S0021-8979(98)05204-9]

I. INTRODUCTION

Since 1984 when the first soft x-ray laser was conclusively demonstrated in Ne-like Se (Refs. 1 and 2) at 20.6 and 20.9 nm, much theoretical and experimental progress has been made for different x-ray lasing schemes. Of the various types of pumping schemes, the collisionally pumped approach has proved to be the most successful and reliable method to produce soft x-ray laser output. Gain saturation of x-ray lasers has been demonstrated in neon-like Zn,[3] Ge,[4] Se,[5] and Y (Ref. 6) and lasing wavelengths as short as 3.5–4.5 nm have been reported using nickel-like Au, W, and Ta.[7] However, the conversion efficiency of generating x-ray lasers from optical pumping lasers is relative low ($\leqslant10^{-6}$) compared with, for example, high order harmonic generation from the same optical lasers.[8]

Using prepulses to enhance the efficiency of generating Ne-like x-ray lasers has been demonstrated successfully in several experiments[9,10] and various multiple pulse irradiation configurations have been investigated.[11,12] Nevertheless, the experimental determination of the optimum pumping pulse configuration is very difficult and time consuming because of the numerous possible variables such as the time interval between pulses and the irradiance levels of the different pulses. Recently, different multiple driving pulse configurations involving short pulses ($\sim$100 ps) have been experimentally examined using neon-like Ni, Cu, Zn, and Ge.[12,13] It was found that when the pulse interval between a prepulse and main pulse is 4.5 ns and the irradiance of the main driving pulse is $\sim1.5\times10^{13}$ W/cm^2, the maximum x-ray laser output for neon-like Zn appears at pulse ratios (prepulse irradiance to main pulse irradiance) of 0.002–0.02. In contrast, when neon-like Ge is pumped by one prepulse and one main pulse separated by 2 ns, the maximum x-ray laser output is at a pulse ratio of 0.1–0.2 when the irradiance of the main pulse is $\sim5\times10^{13}$ W/cm^2. These results suggest that the driving pulse irradiance, pulse interval, and pulse irradiance ratios are critical factors in determining the x-ray laser output and hence efficiency. In order to understand the prepulse effects, some simulations of collisionally pumped x-ray lasers using the double pumping pulse configuration have been reported.[14] However, only simulations where the driving pulse width is $\sim$1 ns with a gain duration of a few hundred picoseconds have been presented.

A new approach for achieving saturated collisional excitation Ne-like x-ray lasing involves pumping by a long prepulse ($\sim$ns) and an ultrashort pulse ($\sim$ few ps).[15] This method has proved successful in generating saturated x-ray lasers in Ne-like Ti and Ge with only $\sim$5 mm plasma length and the results suggest that pulse durations of a few ps may be optimum for pumping collisionally pumped x-ray lasers. However, the necessary chirped pulse amplified (CPA) beam is not widely available on many laser facilities therefore we will restrict the simulations of this paper to pumping pulse durations available without CPA. A pulse duration $\sim$100 ps (as considered in this paper) is often the shortest with sufficient energy available to pump x-ray laser experiments.[13] At the Rutherford Appleton Laboratory, a saturated Ge x-ray laser at 19.6 nm is routinely produced for applications by using double $\sim$100 ps pulse pumping.[16] Recently, saturated x-ray lasing in Ni-like Ag (14 nm),[17] In (12.6 nm), Sn (12 nm) and Sm (7.3 nm)[18] has also been achieved with double $\sim$100 ps pulse irradiation.

In this paper, optimum double short pulse irradiation conditions and the processes producing high x-ray laser output are investigated using the EHYBRID[19] fluid and atomic physics code coupled to a 3D ray tracing postprocessor code.[20] These codes have produced good agreement with recent experimental x-ray laser output.[12,21] We show that the enhancement of x-ray laser output is determined by the level

[a]Electronic mail: jlin@essex.ac.uk
[b]Present address: Department of Physics, University of Kocaeli, Izmit 41000, Turkey.

of the prepulse and the time interval between the prepulse and main pulse. A critical irradiance of the main pulse needed to enable the prepulse techniques to enhance the output is found by varying the intensity of the main driving pulse irradiance. We show that a prepulse in a collisionally pumped x-ray laser can reduce the peak gain coefficient, but usually broadens the spatial gain region because more driving laser energy is absorbed by the laser produced preplasma. The prepulse also causes more shallow electron density gradients and less x-ray refraction which improves the ability of the x-ray laser beam to remain in the gain medium and leads to higher x-ray laser output. An optimum pulse configuration is found as a compromise between the peak gain value, gain width, and the electron density gradients.

II. COMPUTATIONAL MODEL

The computational code used for this study is a modified version of the $1\frac{1}{2}$D hydrodynamic with atomic physics code EHYBRID as described by Holden *et al.*[19] The code models the expansion in the direction away from the target surface with a standard Lagrangian cell geometry, but allows for lateral energy transport by assuming a Gaussian, self-similar density profile in the direction normal to the incoming laser beam and x-ray propagation direction. Energy transport in the direction toward the laser is reduced from the free streaming limit by a flux limit $f=0.1$. The code calculates inverse bremsstrahlung absorption, while resonance absorption is taken into account by dumping 30% of the laser energy at the critical density. The EHYBRID code does not explicitly include other laser-plasma interactions such as Raman and Brillouin scatter and so such laser energy losses are effectively assumed at 50% following Holden *et al.*[19] by only inputting to the code half of the experimental laser energy. In order to model the effects of prepulses at low irradiance, the heating preplasma generated from the cold solid must be treated accurately. The EHYBRID code has consequently been modified by implementing the CHARTD equation of state package.[22]

The electron density and gain profiles from EHYBRID are postprocessed by a 3D ray tracing code[20] to obtain the x-ray laser output. In the 3D ray tracing code, the target is assumed to be pumped by the optical laser in a traveling wave so that the gain profiles calculated by EHYBRID are uniform along the plasma length and not changing in time as the x-ray beam propagates. In order to obtain time integrated results comparable to experimental measurement, several ray tracing calculations at small time intervals during the whole gain duration are necessary. In this paper, the ray tracing calculation is made every 10 ps during the typical gain duration full width at half maximum (FWHM) $\sim$60 ps. Time integrated x-ray laser output is obtained by integrating the area under the fitted profiles of the laser output as a function of time from the ray tracing data points.

III. RESULTS

To evaluate the accuracy of the EHYBRID and ray tracing codes, some complicated multiple pulse pumping x-ray experiment undertaken[23] at the Rutherford Appleton Laboratory have been simulated. The experimental x-ray laser output with different pulse configurations are approximately reproduced by the codes (Fig. 1). The spectra of resonance line emissions have also been simulated using another coprocessor code[24] coupled to EHYBRID. Good agreement between the experimental observations and calculated spectra are found indicating that the EHYBRID code is correctly calculating the plasma ionization balance.

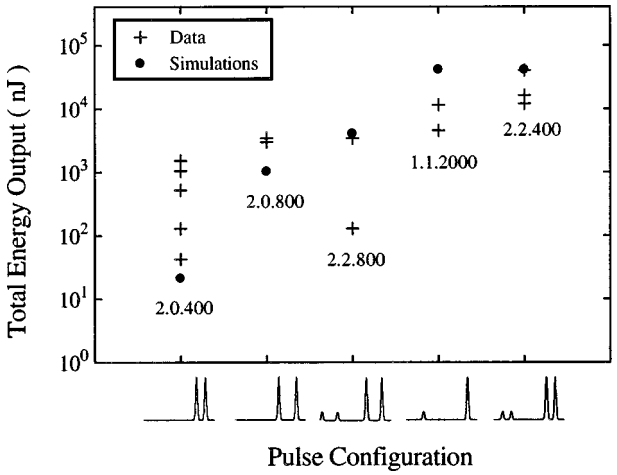

FIG. 1. Comparisons of the simulated x-ray laser output for the neon-like Ge x-ray laser pumped by multiple-pulse irradiation with the experimental output from Warwick *et al.* (Ref. 23). In the 1.1.2000 notation, the first number refers to the number of main pulses, the second to the number of prepulses and the last to the pulse intervals between the main pulses in picoseconds. A schematic variation with time of each pumping configuration is shown under the x-ray laser output points.

The main results presented in this paper refer to Ge slab targets of 1.8 cm length, 100 μm width, and an effectively massive 1 μm thickness. The target is assumed irradiated by a 1.053 μm optical laser of pulse duration 100 ps. The shape of the optical short pulse is assumed to be Gaussian. The driving pulse configurations considered here consist of double pulses with pulse intervals of 800 ps, 2 ns, 3 ns, or 4 ns between the pulses. A simple schematic diagram of the driving pulses is illustrated in Fig. 2. The peak irradiance of the main (second) pulse is usually fixed at 4.75×10^{13} W/cm^2 which means that the energy delivered by the main pulse to the target is $\sim$85 J. The intensity variation of the prepulse (first pulse) is adjusted in the range from 1% to 100% with respect to the main pulse. A typical plot from the

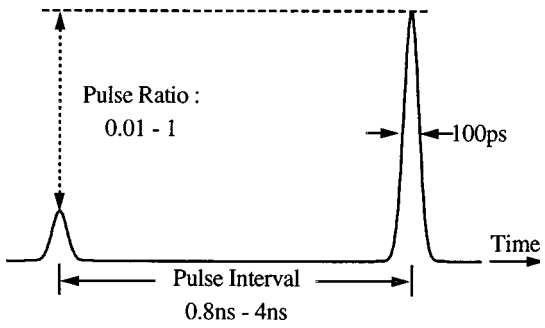

FIG. 2. A schematic plot showing the double driving pulse configuration considered with adjustable pulse ratio and pulse interval.

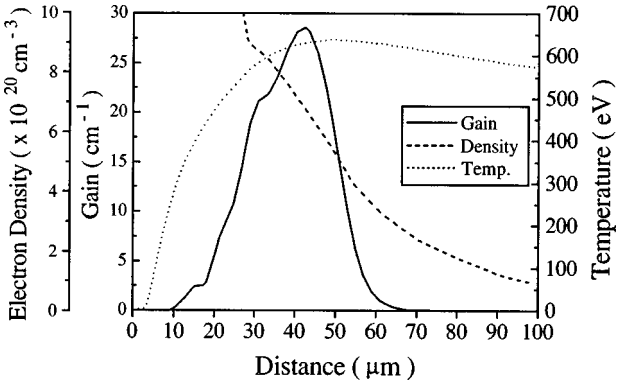

FIG. 3. A typical EHYBRID code output of the electron density, electron temperature, and gain profile after the switching on of the main pulse. This figure is for a Ne-like Ge x-ray laser using double driving pulses with pulse ratio of 0.1 and pulse interval 2 ns at the peak irradiance 4.75 $\times 10^{13}$ W/cm^2 of the main pulse.

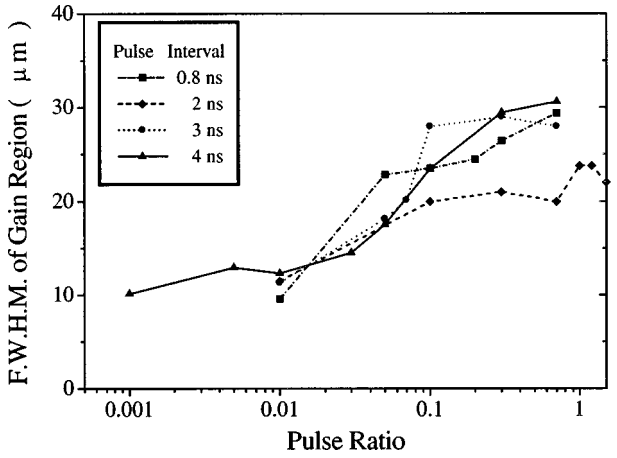

FIG. 5. The spatial width of the gain region (FWHM) at the time when the gain coefficient reaches the maximum value as a function of pulse ratio for various pulse intervals.

output of EHYBRID of the gain profile, electron temperature, and electron density profile after the main pulse switches on is shown in Fig. 3.

With a 2–4 ns delay between prepulse and main pulse, the peak gain coefficient of the double pulse configurations reduces with increasing energy level of the prepulse as shown in Fig. 4. A larger volume of preplasma is generated by a more intense prepulse which results in a larger volume of plasma heated by the following main drive pulse and a broader gain region (Fig. 5). Although a broader gain region is preferred during the amplification, a larger preformed plasma causes the peak gain coefficient to decrease due to a reduced electron temperature as the main pulse irradiance (assumed constant) does not have enough energy to heat the larger volume of preformed plasma. However, with shorter pulse intervals (0.8 ns), the peak gain coefficient increases with increasing prepulse level (see Fig. 4) because the preplasma has not fully expanded within the shorter time interval and thus the electron temperature increases. If the prepulse level continues to increase, more plasma is formed and it expands faster and further and therefore the peak gain falls because of the reduction of the electron temperature. A lower ($<10\%$) prepulse level is optimum for producing gain with longer pulse intervals. Double pulses with a longer pulse interval generally have a lower peak gain because with the longer expansion time, the initial preformed plasma is cooler.

Refraction effects determine the effective gain region which can be sampled by the amplifying x-ray laser beams. Figure 6 shows the electron density gradients at peak gain for the various pulse configurations. It is apparent that the electron density gradient is reduced with increases of the prepulse level as more free electrons are produced with a larger prepulse. With longer delay time between prepulse and the main pulse (2–4 ns), the electrons produced by the two pulses overlap and form a flat density profile. In contrast, if the prepulse level is too low, the electron density profile is only smoothed in the low density region ($<10^{20}$ cm^{-3}), where there is little or no gain. Therefore the higher prepulse level produces less refraction and better amplification. It can also be seen from Fig. 6 that the electron density gradients are not further reduced for pulse intervals longer than 3 ns (compare the 3 and 4 ns pulse interval

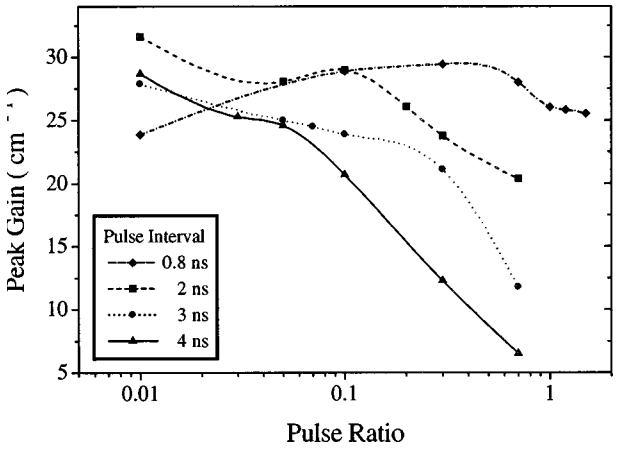

FIG. 4. Variation of the peak gain coefficient for Ne-like Ge 196 Å with a pulse ratio for various pulse intervals.

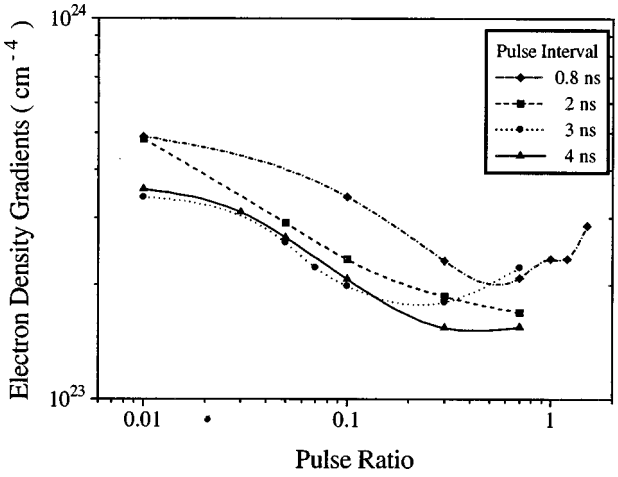

FIG. 6. Variation of electron density gradients with pulse ratio for various pulse intervals. The gradients are the value at the position and time of peak gain coefficient for Ne-like Ge 196 Å.

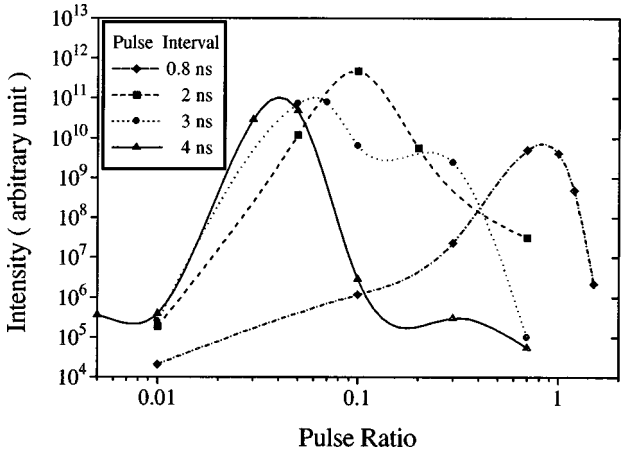

FIG. 7. Variation of Ne-like Ge 196 Å output with pulse ratio for various pulse intervals.

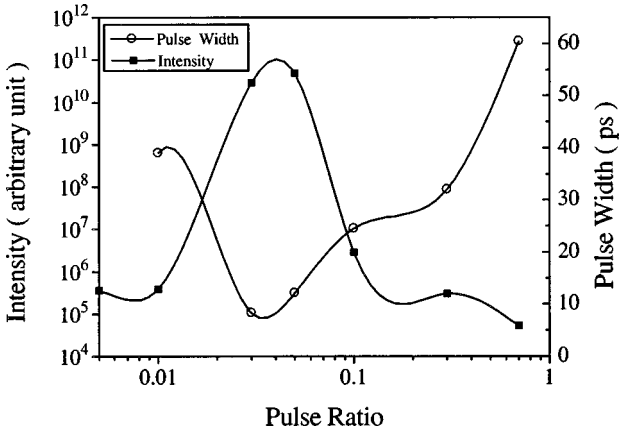

FIG. 8. The relationship between the x-ray laser output intensity and output duration for a driving pulse interval of 4 ns.

curves). The preform plasma simply expands further away from the target surface with a longer pulse interval. This means that the pulse interval is too long, and the advantage of using a prepulse disappears because the peak gain coefficients reduce rapidly (see Fig. 4).

To obtain the maximum laser output, refraction effects have to be minimized and the gain coefficient and the width of gain region maximized. A compromise between the gain and refraction effects determines the final x-ray laser output. Figure 7 shows the laser output with various pulse irradiance as a function of pulse ratio (prepulse/main pulse). It is found that the laser output peaks at lower pulse ratios when the time delay between prepulse and main pulse is longer. This is due to the peak gain dropping faster with pulse ratio in the long pulse interval case. A double pulse with 2 ns time delay at pulse ratio 0.1 gives the maximum output (Fig. 7) because of the relative high peak gain (Fig. 4) and low electron density gradients (Fig. 6).

The pulse duration of the x-ray laser has also been investigated. In Fig. 8, the simulations show an inverse relationship between the x-ray laser output and pulse duration. It is apparent that the higher x-ray laser output coincides with shorter x-ray laser duration. This is similar to the spectral gain narrowing effect produced with a high gain amplification. With a shorter pulse width, the x-ray laser not only produces even higher brightness, but also increases the time-resolving ability for applications.

In order to enhance the efficiency of x-ray lasers, the minimum irradiance required with the main driving pulse for x-ray laser gain has been investigated. With the pulse interval fixed at 4 ns, the x-ray laser output for different irradiances of the main pulse are simulated (Fig. 9). It is apparent that when the main pulse intensity is higher than 4×10^{13} W/cm^2, the prepulse is able to provide several orders of magnitude more intense x-ray laser output than a single pulse irradiance (at 4×10^{13} W/cm^2). In contrast, if the main pulse intensity is reduced to 2 or 3×10^{13} W/cm^2, the advantage of using a prepulse disappears. The intensity of the main pulse is then too low to heat the whole preplasma to reach the required temperature and thus the gain coefficient reduces. The x-ray laser output is reduced even though the electron density gradient is relatively smoother than that for single pulse irradiation.

Other simulations using shorter than 100 ps pulses and the same irradiances as presented here have also been examined. The x-ray laser output decreases with shorter pulses and constant irradiance because the gain region narrows and the electron density gradients are steeper. Reducing the pumping laser pulse duration and keeping the beam energy constant does increase x-ray laser output according to our simulations (in agreement with experiment[12]). However, such simulations are outside the bound of this paper because approximately constant pumping laser energy as the laser pulse duration is reduced can only be achieved, in practice, with CPA pulse compression techniques and here, the purpose is to consider the simple non-CPA pumping pulses.

IV. DISCUSSION

Simulations predict that the optimum pulse ratio for maximum x-ray laser output is not sensitive to the irradiance of the main pumping pulse (Fig. 9). However, in Fig. 7, the optimum pulse ratio varies as the time interval between the

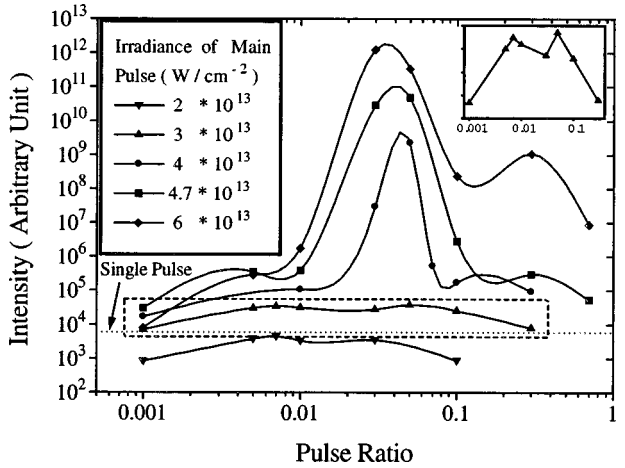

FIG. 9. Ge x-ray laser output for various peak irradiances of the main pulse as a function of pulse ratio. The inset shows a linear plot of the x-ray laser output for a peak irradiance close to the threshold for lasing of 3×10^{13} W/cm^2 as a function of the pulse ratio.

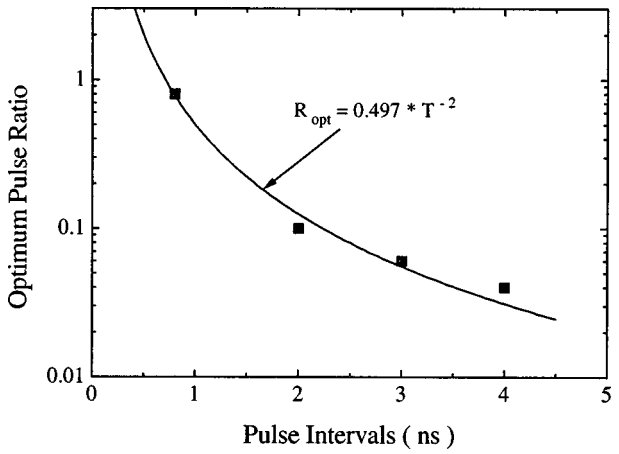

FIG. 10. The simulated optimum pulse ratio for maximum Ne-like Ge x-ray laser output at 196 Å as a function of the pulse intervals (data points) with a fitting function proportional to the inverse square of the pulse intervals (solid curve shown).

prepulse and main pulse is changed. It is found that the optimum pulse ratio scales as T^{-2}, where T is the pulse interval (see Fig. 10). This can be explained in terms of the thermal energy density required to balance the effects of the varying gain coefficient, the width of the gain region, and refraction due to the electron density gradients. We quantify the thermal energy density by the parameter T_e/V_{pre}, where T_e is the peak electron temperature during the main pulse and V_{pre} is the volume of the preplasma just before arrival of the main pulse. Simulations show that the optimum thermal energy density is constant for the parameter range investigated in this paper. A higher thermal energy density than the optimum implies overionization or a narrow gain region with steep electron density gradients, while a lower thermal energy density than the optimum gives low gain and thus lower laser output.

If we assume the density profile in the double pulse pumping is determined by the prepulse because of the relative long pulse interval compared with the pulse duration, the role of the following main pulse can be assumed only to heat the preformed plasma. The number of electrons produced by the prepulse is proportional to $(\nu \times t)^2$, where ν is the ionic sound speed and t is the prepulse duration. The plasma scale length before switching on the main pulse is proportional to $\nu \times T$. This gives the volume of the two-dimensionally expanding preplasma $V_{pre} \sim \nu^2 T^2$ (expansion along the direction of the line focus is assumed to be negligible). By assuming the relation between the ionic sound speed and the prepulse irradiance is $\nu \propto I_{pre}^a$, where a is a constant to be determined, the lasing electron temperature can then be represented as $T_e \propto I_{\text{main}}/I_{pre}^{2a} \cdot t^2$, where I_{main} is the main pulse irradiance. Hence, the optimum thermal energy density $T_e/V_{pre} \propto I_{\text{main}} I_{pre}^{-4a} t^{-2} T^{-2}$. If the prepulse energy is absorbed by resonance absorption, a simple balance between $P\nu$ and the laser irradiance I_{pre}, where P is the plasma pressure at the critical density gives that $\nu \propto I_{pre}^{1/3}$.[25] If the prepulse energy is mainly absorbed by inverse bremsstrahlung, we may expect $\nu \propto I_{pre}^{2/9}$.[26] However, it is found that if $a = 0.25$, this gives the optimum pulse ratio $(I_{pre}/I_{\text{main}})_{opt} \propto t^{-2} T^{-2}$, which agrees with the scaling equation in Fig. 10. This suggests that resonance absorption and inverse bremsstrahlung absorption are both playing important roles during the prepulse interaction with the target. It is also interesting to see that the simple model predicts that the optimum ratio decreases as the prepulse duration t increases. This is due to a longer prepulse ablating more material from the target which causes the peak temperature during the main pulse to drop.

V. CONCLUSION

Simulations have shown how a prepulse which precedes the main pulse by a few ns can modify a laser produced plasma medium during the main pulse and produce more x-ray laser output. Higher prepulse levels produce lower peak gain coefficients, but broader gain regions. An optimal prepulse level is found because a larger prepulse gives lower electron density gradients which allow the laser beam to propagate better in the gain region. The simulations have shown that the maximum output of the double pulse configuration is reached at a lower pulse ratio as the pulse interval is increased. The optimal double pulse configuration is for double pulses separated by 2 ns at pulse ratio ~ 0.1.

The simulations predict that the threshold irradiance of the main pulse for prepulse effects to show orders of magnitude enhancement of output is around $3-4 \times 10^{13}$ W/cm^2 for Ne-like Ge. This may explain why some experiments[13] cannot find an apparent optimum driving pulse ratio. The intensity of the main drive pulse in these cases may be close to or under the relevant threshold value. The simulation results can be explained by a simple theory which predicts that the optimum pulse ratio scale as the inverse square of the prepulse duration and the inverse square of the pulse interval.

ACKNOWLEDGMENTS

This work was supported by the United Kingdom Science and Engineering Research Council and Ministry of Defence. J.Y.L. acknowledges an Overseas Research Students Awards from the Committee of Vice-Chancellors and Principals of the Universities of the United Kingdom.

[1] D. L. Matthews, P. L. Hagelstein, M. D. Rosen, M. J. Eckart, N. M. Ceglio, A. U. Hazi, H. Medecki, B. J. MacGowan, J. E. Trebes, B. L. Whitten, E. M. Campbell, C. W. Hatcher, A. M. Hawryluk, R. L. Kauffman, L. D. Pleasance, G. Rambach, J. H. Scofield, G. Stone, and T. A. Weaver, Phys. Rev. Lett. **54**, 110 (1985).
[2] M. D. Rosen, P. L. Hagelstein, D. L. Matthews, E. M. Campbell, A. U. Hazi, B. L. Whitten, B. J. MacGowan, R. E. Turner, and R. W. Lee, Phys. Rev. Lett. **54**, 106 (1985).
[3] P. Jaegle, A. Carillon, P. Dhez, P. Goedkindt, G. Jamelot, A. Klisnick, B. Rus, P. Zeitoun, S. Jacqemot, D. Mazataud, A. Mens, and C. Chauvineau, AIP Conf. Proc. **332**, 25 (1994).
[4] A. Carillon, H. Z. Chen, P. Dhez, L. Dwivedi, J. Jacoby, P. Jaegle, G. Jamelot, J. Zhang, M. H. Key, A. Kidd, J. P. Raucourt, G. J. Tallents, and J. Uhomoibhi, Phys. Rev. Lett. **68**, 2917 (1992).
[5] J. A. Koch, B. J. MacGowan, L. B. Da Silva, D. L. Matthews, J. H. Underwood, P. J. Batson, and S. Mrowka, Phys. Rev. Lett. **68**, 3291 (1992).
[6] L. B. Da Silva, B. J. MacGowan, S. Mrowka, J. A. Koch, R. A. London, D. L. Matthews, and J. H. Underwood, Opt. Lett. **18**, 1174 (1993).
[7] B. J. MacGowan, S. Maxon, L. B. Da Silva, D. J. G. Fields, C. J. Keane,

D. L. Matthews, A. L. Osterheld, J. H. Scofield, G. Shimkaveg, and G. F. Stone, Phys. Rev. Lett. **65**, 420 (1990).
[8] P. A. Norreys, M. Zepf, S. Moustaizis, A. P. Fews, J. Zhang, P. Lee, M. Bakarezos, C. N. Danson, A. Dyson, P. Gibbon, P. Loukakos, D. Neely, F. N. Walsh, J. S. Wark, and A. E. Dangor, Phys. Rev. Lett. **76**, 1832 (1996).
[9] J. Nilsen, B. J. MacGowan, L. B. Da Silva, and J. C. Moreno, Phys. Rev. A **48**, 4682 (1993).
[10] G. F. Cairns, C. L. S. Lewis, M. J. Lamb, A. G. MacPhee, D. Neely, P. Norreys, M. H. Key, S. B. Healy, P. B. Holden, G. J. Pert, J. A. Plowes, G. J. Tallents, and A. Demir, Opt. Commun. **123**, 777 (1996).
[11] J. Nilsen and J. C. Moreno, Phys. Rev. Lett. **74**, 3376 (1995).
[12] A. Behjat, J. Lin, G. J. Tallents, A. Demir, M. Kurkcuoglu, C. L. S. Lewis, A. G. MacPhee, S. P. McCabe, P. J. Warwick, D. Neely, E. Wolfrum, S. B. Healy, and G. J. Pert, Opt. Commun. **135**, 49 (1997).
[13] A. G. MacPhee, C. L. S. Lewis, P. J. Warwick, I. Weaver, A. Demir, M. Holden, J. Krishnan, G. J. Tallents, P. Goedkindt, P. Jaegle, G. Jamelot, A. Klisnick, M. Nantel, B. Rus, and Ph. Zeitoun, Opt. Commun. **133**, 525 (1997).
[14] S. B. Healy, G. F. Cairns, C. L. S. Lewis, G. J. Pert, and J. A. Plowes, IEEE J. Sel. Top. Quantum Electron. **1**, 949 (1995).
[15] S. B. Healy, K. A. Janulewicz, J. A. Plowes, and G. J. Pert, Opt. Commun. **132**, 442 (1996); P. V. Nickles, M. Schnürer, M. P. Kalashnikov, W. Sandner, V. N. Schlyaptsev, C. Danson, D. Neely, E. Wolfrum, J. Zhang, A. Behjat, A. Demir, G. Tallents, P. J. Warwick, and C. L. S. Lewis, Proc. SPIE **3156**, 80 (1997).
[16] J. Zhang, P. J. Warwick, E. Wolfrum, M. H. Key, C. Danson, A. Demir, S. B. Healy, D. H. Kalantar, N. S. Kim, C. L. S. Lewis, J. Lin, A. G. MacPhee, D. Neely, J. Nilsen, G. J. Pert, R. Smith, G. J. Tallents, and J. S. Wark, Phys. Rev. A **54**, R4653 (1996); D. H. Kalantar, M. H. Key, L. B. Da Silva, S. G. Glendinning, B. A. Remington, J. E. Rothenberg, F. Weber, S. V. Weber, E. Wolfrum, N. S. Kim, D. Neely, J. Zhang, J. S. Wask, A. Demir, J. Lin, R. Smith, G. J. Tallents, C. L. Lewis, A. McPhee, J. Warwick, and J. P. Knauer, Phys. Plasmas **4**, 1985 (1997).
[17] J. Zhang, A. G. MacPhee, J. Nilsen, J. Lin, T. W. Barbee, Jr., C. Danson, M. H. Key, C. L. S. Lewis, D. Neely, R. M. N. O'Rourke, G. J. Pert, R. Smith, G. J. Tallents, J. S. Wark, and E. Wolfrum, Phys. Rev. Lett. **78**, 3856 (1997).
[18] J. Zhang, A. G. MacPhee, J. Lin, E. Wolfrum, R. Smith, C. Danson, M. H. Key, C. L. S. Lewis, D. Neely, J. Nilsen, G. J. Pert, G. J. Tallents, and J. S. Wark, Science **276**, 1097 (1997).
[19] P. B. Holden, S. B. Healy, M. T. M. Lightbody, G. J. Pert, J. A. Plowes, A. E. Kingston, E. Robertson, C. L. S. Lewis, and D. Neely, J. Phys. B **27**, 341 (1994).
[20] J. A. Plowes, G. J. Pert, S. B. Healy, and D. T. Toft, Opt. Quantum Electron. **28**, 219 (1996).
[21] J. A. Plowes, G. J. Pert, and P. B. Holden, Opt. Commun. **116**, 260 (1995).
[22] S. L. Thompson and H. S. Lauson, Sandia Laboratories, paper SS-RR710714 (1975).
[23] P. J. Warwick, A. Bejhat, M. Kurkcuoglu, C. L. S. Lewis, A. G. MacPhee, S. McCabe, D. Neely, G. J. Tallents, and E. Wolfrum, Opt. Commun. **144**, 192 (1997).
[24] G. J. Tallents, J. Y. Lin, A. Demir, A. Behjat, J. Zhang, E. Wolfrum, J. Wark, M. H. Key, C. L. S. Lewis, A. MacPhee, S. P. McCabe, P. J. Warwick, D. Neely, S. Healy, G. J. Pert, P. V. Nickles, M. Kalashnikov, and M. Schnürer, Proc. SPIE **3156**, 30 (1997).
[25] C. Fauquignon and F. Floux, Phys. Fluids **13**, 386 (1970).
[26] H. Puell, Z. Naturforsch. **25a**, 1807 (1970).